

Detecting the Liquid–Solid Contact Electrification Charges in a Liquid Environment


Published as part of *The Journal of Physical Chemistry virtual special issue “125 Years of The Journal of Physical Chemistry”*.

Shiquan Lin, Mingli Zheng, and Zhong Lin Wang*

 Cite This: <https://doi.org/10.1021/acs.jpcc.1c03483>

 Read Online

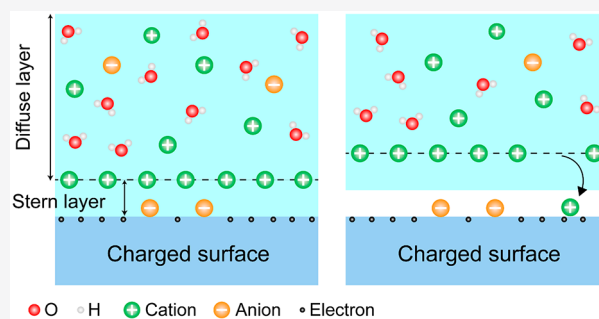
ACCESS |

 Metrics & More

 Article Recommendations

 Supporting Information

ABSTRACT: Contact electrification (CE) has been known for more than 2600 years, but its mechanism remains ambiguous, especially for liquid–solid cases. In previous studies on liquid–solid CE, the charges on a dielectric surface in a liquid environment have not been discussed due to the lack of proper measurement techniques, which may be responsible for the poor understanding on the liquid–solid CE. Here, the CE between dielectrics and different liquids, including deionized (DI) water, benzene, and cyclohexane (CYH), is performed by using dual harmonic Kelvin probe force microscopy (DH-KPFM). We focus on the transferred charges on the dielectric surface when it keeps in contact with a liquid. It is observed that the CE surface charges are screened in DI water, but not in organic solutions, suggesting that the electric double layer (EDL) is responsible for the screening of the surface charges. Moreover, it is revealed that the charge transfer in liquid–solid CE occurs not only in the contact but also during the separation process. Based on the observations, a model is proposed to describe the whole process of liquid–solid CE, in which the electron transfer plays a dominant role, and the adsorption of counterions in the EDL on the dielectric surface during separation is considered.



INTRODUCTION

Contact electrification (CE) is one of the most common physical phenomena, but its mechanism is still under debate, especially for liquid–solid cases. Most of the previous studies have focused on solid–solid CE; the identity of charge carriers has been widely discussed.¹ It is also revealed that the CE can occur at liquid–liquid interfaces.² In recent years, liquid–solid CE has attracted more and more attention because of the invention of the liquid–solid triboelectric nanogenerator (L-S TENG) for energy harvesting.^{3–9} A regular liquid–solid CE consists of two steps. The liquid first contacts the solid surface and then separates with the solid surface, generating the surface static charges. Previous studies about liquid–solid CE focused on the transferred charges left on the solid surface after the contact with a liquid,^{10–13} while the amount of charges on the solid surface when it is in contact with the liquid was rarely measured. The lack of a sufficient understanding of the first step in liquid–solid CE (liquid and solid in contact) may be a main reason the mechanism of liquid–solid CE is ambiguous. Moreover, in some energy conversion techniques based on charge transfer at the liquid–solid interface, such as the streaming current generator,^{14,15} electrokinetic energy device,¹⁶ fiber-shaped fluidic nanogenerator (FFNG),¹⁷ carbon–water device,¹⁸ and so on, the liquid keeps in contact with the

solid surface. Therefore, it is of both scientific and technical implications to measure the surface charges of a solid when it is in contact with a liquid.

The lack of proper techniques for measuring the surface charges in liquid environment may be responsible for the poor understanding of the charge transfer when the liquid and solid are in contact. Kelvin probe force microscopy (KPFM) was proven to be a powerful tool for measuring the charge density on a solid surface in air conditions.^{19–21} But unfortunately, it cannot be used in a liquid environment directly, especially in polar liquids and conductive liquids, since that direct (DC) voltage bias needs to be applied to compensate for the potential difference between the tip and the sample, which may lead to the electric double-layer (EDL) charging, migration of the ions in liquid, and even decomposition of the liquid molecules. To overcome this problem, recently dual-harmonic Kelvin probe force microscopy (DH-KPFM) was designed to

Received: April 18, 2021

Revised: May 18, 2021

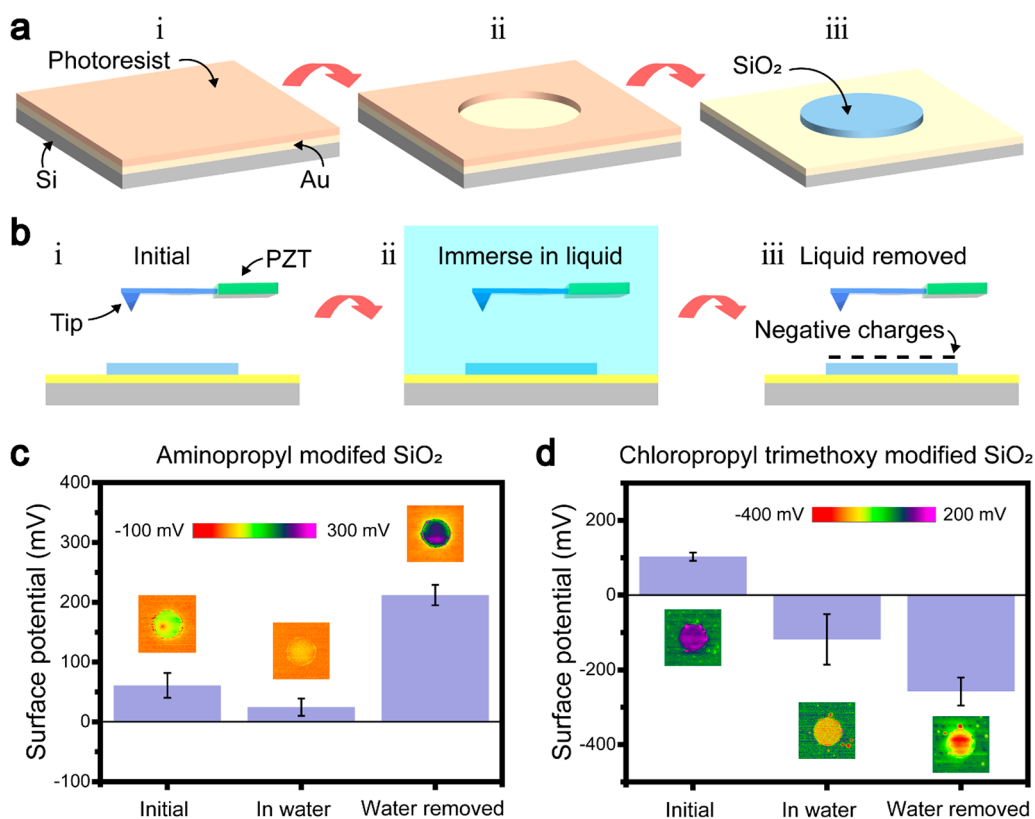


Figure 1. Schematic illustration of the sample preparation and liquid–solid CE experiments. (a) Fabrication process of the samples. (b) Measurement of the sample surface potential in different steps of liquid–solid CE (before contact, in contact, and after contact). Results of the surface potential measurement in different steps of CE (c) between aminopropyl modified SiO₂ and DI water (d) and that between chloropropyltrimethoxy modified SiO₂ and DI water.

measure the surface potential of the solid in a liquid environment.^{22,23} As with the conventional KPFM, the vibration of the cantilever is also excited by the alternating (AC) voltage bias applied between the tip and the sample in DH-KPFM. But the difference is that the amplitudes of the cantilever at the resonant frequency (ω) and twice the resonant frequency (2ω) are both recorded for further calculating the surface potential of the solid, and the DC bias is not required in DH-KPFM. Though the AC bias may also lead to the EDL charging, it was demonstrated that it can be avoided by increasing the frequency of the AC bias, which makes the mobile ions in quasi-static equilibrium²⁴ so that the DH-KPFM can be successfully operated under a liquid.

In this paper, the CE between different solid samples and liquids, including deionized (DI) water, benzene, and cyclohexane (CYH), was performed. The surface potential of the samples before contact, in contact, and after contact with the liquids was measured by using DH-KPFM. The EDL at the liquid–solid interface was detected by using the force curve method. It was found that the charge transfer occurs when the liquid contacts the solid surface, and the surface charges will be screened by the EDL at the interface. It was suggested that the counterions in the EDL may attach on the solid surface during separation and reduce the net static charges left on the surface. Moreover, the thermionic emission experiments implied that the charge transfer between liquid and solid may be mainly caused by electron transfer.

METHODS

The sample preparation process is shown in Figure 1a. The Au film and photoresist film were deposited on a polished silicon surface (i). Then, a circular region with a diameter of 10 μm on the photoresist was removed (ii). In the final step, a 50 nm thin insulator film, such as SiO₂ film, was further deposited on the sample; a circular insulator film sample was obtained (iii), and its topography is shown in Figure S1. The experiments of CE between the sample and liquid are shown in Figure 1b. The initial surface potential of the sample was first measured by using the DH-KPFM with a conductive tip (i). Then, the tip and the sample were both immersed into liquid, and the surface potential of the solid was measured in a liquid environment (ii). In the third step, the liquid was removed from the solid surface, and the surface potential of the solid was measured in air conditions again (iii). We noticed that the change of the surface potential of the Au was limited before and after contact with DI water so that the surface potential of the Au can be treated as a background potential, and the change in the surface potential of the circular insulator film relative to the background potential is caused by the triboelectric charges on the insulator film surface. The details of the experiments are given below.

Sample Preparations. The Au and photoresist layer were deposited on a highly doped silicon wafer by electron beam evaporation and spin-coating, respectively. The dielectric films, including SiO₂, Si₃N₄, and Al₂O₃, were deposited by magnetron sputtering.

KPFM Measurements. The experiments were performed on a commercial atomic force microscope (Dimension Icon,

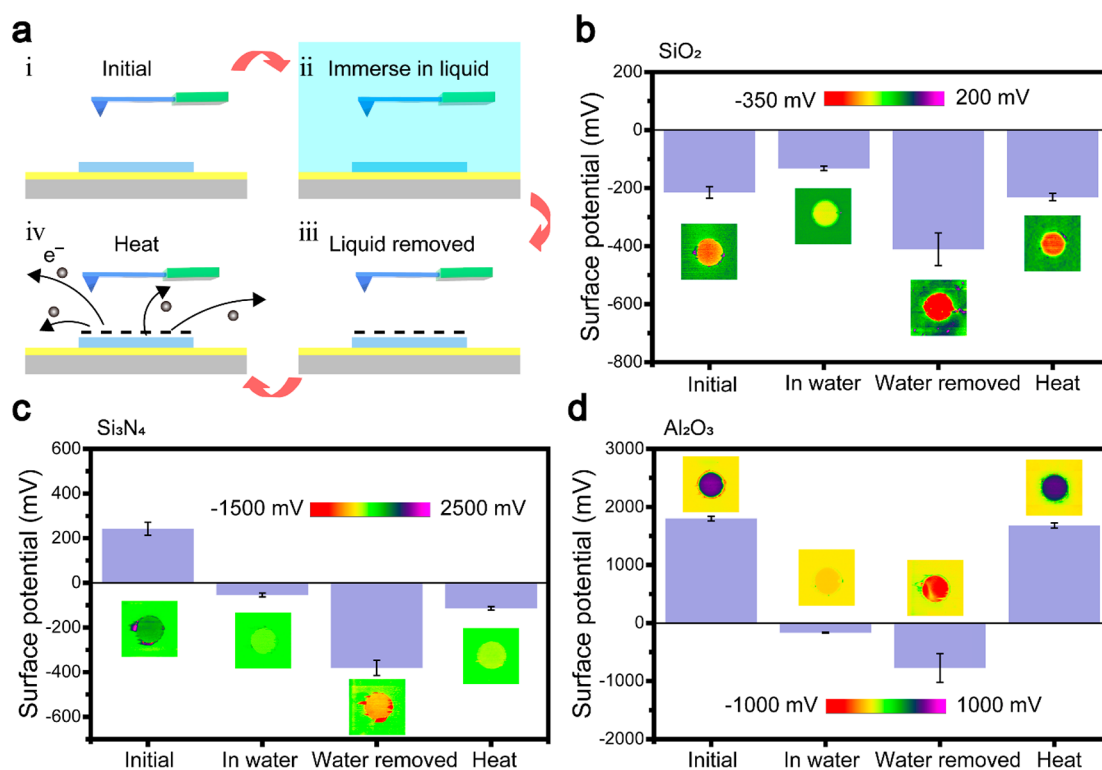


Figure 2. Contact electrification between DI water and different dielectrics. (a) Measurement the sample surface potential in different steps of liquid–solid CE (before contact, in contact, and after contact) and thermionic emission experiment (at 433 K for 10 min). Results of thermionic emission experiments and CE between (b) SiO₂, (c) Si₃N₄, and (d) Al₂O₃ and DI water.

Bruker, USA). A SCM-PIT (Bruker, USA; Pt coated; spring constant: 2.8 N/m; resonant frequency in air: 55 kHz; resonant frequency in DI water: 23 kHz) was used as the conductive tip in the DH-KPFM measurement. In the DH-KPFM measurement, an AC bias was applied between the tip and the sample to excite the cantilever vibration at its resonant frequency. The amplitudes of the cantilever at resonant frequency (ω) as well as twice the resonant frequency (2ω) and the phase of vibration were all recorded, and the surface potential was further calculated according to previous studies.²² In the DH-KPFM scanning, the scan size was 20 μ m, and the lift height was set to 100 nm. In air conditions, the amplitude of the AC drive bias was set to 5 V. When the HD-KPFM was operated in a liquid environment, the amplitude of the AC drive bias was set to 500 mV.

RESULTS AND DISCUSSION

The CE between the functional group modified SiO₂ and DI water was first investigated to test the experimental method, and the results are shown in Figure 1c,d. The initial surface potential of the aminopropyl modified SiO₂ was about 60 mV. When it was immersed into DI water, the surface potential of the aminopropyl modified SiO₂ decreased to about 25 mV. The surface potential increased to 200 mV when the DI water was removed from the sample surface. The change of the sample surface potential before and after the contact with DI water was positive in the experiments, which implies that the aminopropyl modified SiO₂ received positive charges in the contact with DI water. This is because that the electron affinity of the aminopropyl is low, and it prefers to donate electrons in the CE, which is consistent with previous studies.¹³ Because the aminopropyl modified SiO₂ received positive charges when

it contacts with DI water, the decreasing of the surface potential when it was immersed into DI water can only be due to the screening effect of the EDL on the surface positive charges. The results of the CE between chloropropyltrimethoxy modified SiO₂ and DI water are given in Figure 1d. Note that the surface potential of the sample changed from 100 to -110 mV when it was immersed into DI water, which suggests that the chloropropyltrimethoxy modified SiO₂ received negative charges in the contact with DI water. It is easy to understand this result since the chloropropyltrimethoxy has a high electron affinity and is more likely to receive electrons in the CE.¹³ When the DI water was removed, the surface potential of the sample became more negative, which implies the screening effect of the EDL on the surface charges. These two experiments successfully demonstrated that the DH-KPFM can be used to measure the surface potential of solid in liquid environments, and the screening effect of the EDL on the surface charges was observed.

Different dielectric films, including unmodified SiO₂, Si₃N₄, and Al₂O₃, were used to contact the DI water in the CE experiments. The identity of the charge carriers was always of concern in the CE, so that the thermionic emission experiments were performed after the DI water was removed to distinguish the electron transfer and ion transfer in the CE,¹⁰ as shown in Figure 2a. Figure 2b gives the surface potential of the unmodified SiO₂ in different steps of CE (before contact, in contact, and after contact) and after the thermionic emission experiment. The initial surface potential of the SiO₂ sample was about -200 mV, and it decreased to -120 mV when the SiO₂ was immersed in DI water. When the DI water was removed, the SiO₂ surface potential increased to -400 mV, which means it received negative charges in the CE.

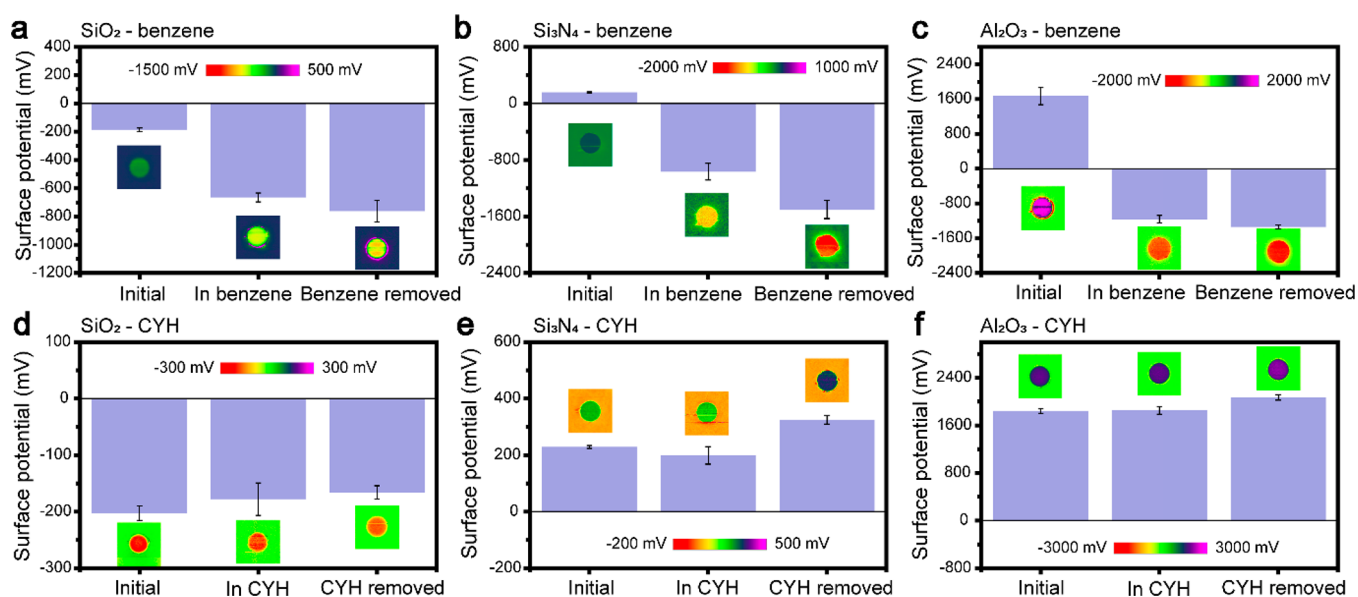


Figure 3. Contact electrification between different organic solutions and different dielectrics. Results of the surface potential measurement in different steps of CE between (a) SiO_2 , (b) Si_3N_4 , and (c) Al_2O_3 and benzene and that between (d) SiO_2 , (e) Si_3N_4 , and (f) Al_2O_3 and cyclohexane (CYH).

The surface potential was found to recover to its original value (-200 mV) after the sample was heated at 473 K for 10 min (the electrons will be removed in this process).¹⁰ This means that the transferred negative charges from the DI water to the SiO_2 surface in the CE were mainly electrons. For the CE between Si_3N_4 , Al_2O_3 , and DI water (Figure 2c,d), the surface potential of the solid samples reversed from positive to negative when they were immersed into DI water, and the negative surface potential further increased when the DI water was removed. It means that Si_3N_4 and Al_2O_3 both receive negative charges in the contact with the DI water, which is consistent with previous studies in which the DI water was demonstrated to occupy a very positive position in the triboelectric series.²⁵ When the samples were heated at 473 K for 10 min, the surface potential of Al_2O_3 returned to its initial value and that of the Si_3N_4 became more positive, but it remained on negative. This suggests that the charge transfer between Al_2O_3 and DI water is mainly caused by electron transfer, and both electron transfer and ion transfer occurred in the CE between the Si_3N_4 sample and the DI water. It should be noticed that the ratio of the electron transfer and ion transfer in the CE here is different than that in previous studies; this is because that the sample history in these two works was different, which can affect the CE significantly.²⁶ The CE between DI water and different dielectrics shows that the electron transfer plays a dominant role in the liquid–solid CE. The transferred electrons on the solid surface will be screened by the EDL when the solid is immersed in DI water.

The screening of the triboelectric charges on the solid surface is usually a problem that needs to be avoided in the TENGs, especially for TENGs for harvesting water wave energy. It is well accepted that the surface charges are screened by the counterions in the EDL at the liquid side. This implies that if the organic solutions, which do not contain ions, are used as the liquid contact pair, the triboelectric charges on the solid surface will not be screened. Here, the benzene and CYH were used as the liquid in the CE experiments, and the results are shown in Figure 3. It can be seen that the SiO_2 , Si_3N_4 , and

Al_2O_3 samples were all negatively charged in the contact with benzene (Figure 3a–c). Because there are not any ions in benzene, the triboelectric charges on the sample surfaces should be electrons. Moreover, the electrons may come from the delocalized π bond of the benzene. When the benzene was removed, the surface potential of the sample was not significantly changed compared to that when the liquid was DI water (Figure 2). This means that the charges on the dielectric surfaces were not screened in the benzene environment. In the CE between the dielectrics and the CYH, the dielectrics were found to be slightly positively charged, which is consistent with previous studies, and the screening of the surface charges by EDL was also not observed.

These results provide a strategy for TENG encapsulation. The TENG package can be filled with organic solutions to keep water out and avoid the screening of the triboelectric charges on the solid surface. To further verify this strategy, a biased conductive tip was used to scan the SiO_2 sample in different liquid environments for generating the triboelectric charges on the surface, and the surface potential was measured under liquid; the results are shown in Figure S2. It is shown that no charges were detected when the SiO_2 was in DI water and benzene. The triboelectric charges in the DI water were screened, and that in the benzene may escape from the surface through the delocalized π bond in benzene. The results indicate that the CYH is a suitable organic liquid to protect the TENG from the effect of charge screening. The injected charges were trapped well on the SiO_2 surface in the CYH environment.

The screening of the solid surface charges in the DI water by the EDL is not surprising. However, we noticed that the charges left on the solid surface when the water was removed did not simply depend on the surface potential of the solid under DI water (in contact). For example, the surface potentials of the SiO_2 and Si_3N_4 were both about -400 mV after the water was removed, but the surface potential of the SiO_2 was significantly higher than that of the Si_3N_4 under water (Figure 2). This may be caused by the different screening

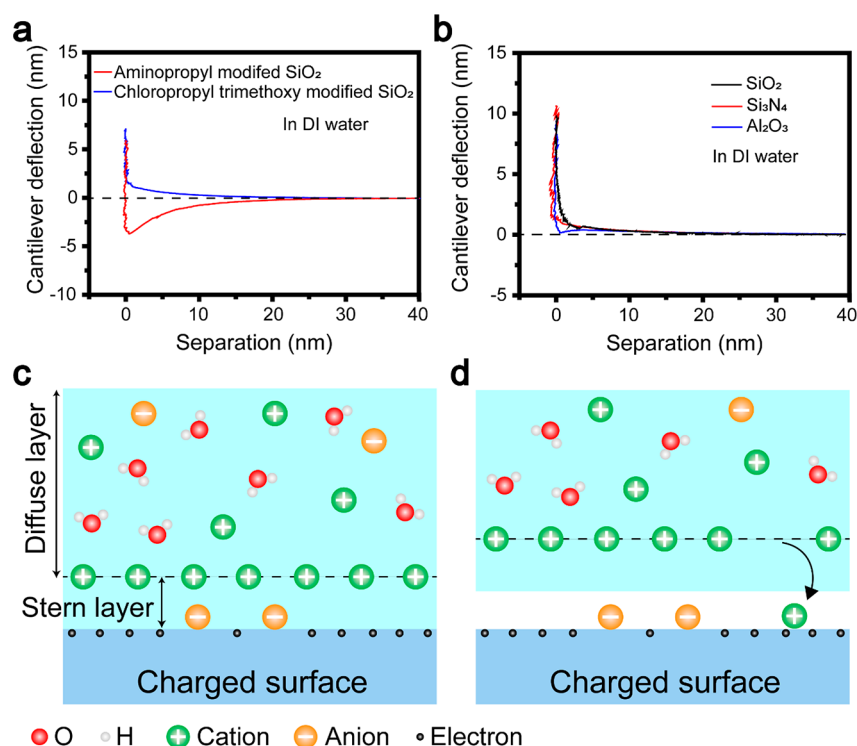


Figure 4. Detecting the electric double layer at the liquid–solid interface. The deflection–separation relation when the Si_3N_4 tip approaches (a) aminopropyl modified and chloropropyltrimethoxy modified SiO_2 surfaces in DI water. The deflection–separation relation when the Si_3N_4 tip approaches (b) SiO_2 , Si_3N_4 , and Al_2O_3 surfaces in DI water. Schematic of the electric double layer at the liquid–solid interface (c) in contact and (d) during separation.

strength of DI water to the charges on different dielectric surfaces or that the charge transfer between the DI water and the dielectric solids not only occurs when they come into contact but also occurs during separation. The latter explanation is more reasonable because the solid surface charges are screened by the EDL, which depends on the liquid side rather than the solid side at the interface. To verify this statement, the EDL structures at the liquid and solid interface were detected by using the force curve method here,²⁷ and a Si_3N_4 tip was used in the force curve experiments. The Si_3N_4 tip will be negatively charged when it is immersed into DI water. If the negatively charged Si_3N_4 tip approaches a charged solid surface, the tip will be subjected to an electrostatic force and the cantilever will be deflected. Because of the screening effect of the EDL, the charged Si_3N_4 tip can only feel the surface charges when it enters the diffuse layer of the EDL. As shown in Figure 4a, a repulsive force was generated on the Si_3N_4 tip when it approached the chloropropyltrimethoxy modified SiO_2 surface, and the separation between the tip and the sample surface was <20 nm. This is because both the Si_3N_4 tip and the chloropropyltrimethoxy modified SiO_2 surface were negatively charged in DI water, and the thickness of the EDL was 20 nm. When the Si_3N_4 tip approached the aminopropyl modified SiO_2 surface, which was positively charged in DI water, an attractive force was generated on the tip, and the threshold tip–sample separation was also 20 nm. As expected, the EDLs on different solid surfaces were 20 nm thick, as shown in Figure 4b. A similar EDL structure should correspond to the same screening strength.

Therefore, it is suggested that the charge transfer in liquid–solid CE occurs during the separation of the liquid and solid. Here, we propose a model to describe the whole process of

liquid–solid CE according to the observations. As shown in Figure 4c, when the aqueous solution contacts a dielectric surface, the electrons will transfer at the interface due to the overlap of the electron clouds of the atoms.^{28–30} As a result of the electrostatic interaction, the counterions are attracted to the surface, forming an EDL, which has been described in Wang’s hybrid layer model.³¹ When the solution separates from the solid surface, some counterions in the EDL may attach to the solid surfaces, especially the counterions in the Stern layer, which are very close to the surface (Figure 4d). The attachment of the counterions will reduce the net transferred triboelectric charges on the solid surface. This model provides an explanation for the small amount of charge transfer on hydrophilic surface in liquid–solid CE³² because the liquid is difficult to be completely removed from a hydrophilic surface and the adsorption of counterions on the charged surface is difficult to avoid.

In recent years, the mechanism of the liquid–solid CE has been discussed intensively around the identity of charges carriers, electron transfer, or ion transfer.³¹ More and more experimental evidence supports that both the electron transfer and ion transfer occur in the liquid–solid CE, and electron transfer plays a dominant role in some cases.^{10,11} Based on the electron transfer at the liquid–solid interface, the formation of EDL was revisited, and Wang’s hybrid model was proposed,³¹ in which the electron transfer is considered as the first step in the formation of the EDL. The discovery in this work completes the current theory for liquid–solid CE, in which the charge transfer during the liquid–solid separation was not considered. It was demonstrated that the electron transfer in liquid–solid CE is due to the overlap of the electron clouds,^{28–30} and the ion transfer is caused by the ionization

reactions. Here, we find that adsorption of the counterions in the EDL is another pathway for ion transfer. The adsorption of the counterions provides an explanation for the different polarity of the transferred electrons and transferred ions on a solid surface in liquid–solid CE, which was reported in previous studies.¹⁰

CONCLUSIONS

In conclusion, the liquid–solid CE was investigated by using DH-KPFM at the microscale. A highlight of this work is that the surface potential of the charged dielectrics was measured in a liquid environment. By comparison of the surface potential of the dielectrics in DI water and that after the DI water was removed, it was revealed that the triboelectric charges on the dielectric surface will be significantly screened by the DI water. When the organic liquids, including benzene and CYH, were used as the liquid contact pairs, the screening of the triboelectric charges was not observed. This result provides a strategy for TENG encapsulation in that the TENG package can be filled with organic solutions to avoid the screening of the triboelectric charges in CE. Moreover, the data indicate that the charge transfer can occur not only when the liquid contacts the dielectric but also during the separation of the liquid after contacting the dielectric, which was rarely considered in previous studies on the liquid–solid CE. Though electron transfer was demonstrated to play a dominant role in liquid–solid CE by the thermionic emission experiments, the ion transfer in liquid–solid CE cannot be ignored. The findings in this work suggest that ion transfer in liquid–solid CE comes not only from the ionization reactions but also from the adsorption of the counterions in the EDL.

ASSOCIATED CONTENT

Supporting Information

The Supporting Information is available free of charge at <https://pubs.acs.org/doi/10.1021/acs.jpcc.1c03483>.

Additional data of the experiments (PDF)

AUTHOR INFORMATION

Corresponding Author

Zhong Lin Wang – Beijing Institute of Nanoenergy and Nanosystems, Chinese Academy of Sciences, Beijing 100083, P. R. China; School of Materials Science and Engineering, Georgia Institute of Technology, Atlanta, Georgia 30332–0245, United States; orcid.org/0000-0002-5530-0380; Email: zlwang@binn.cas.cn

Authors

Shiquan Lin – Beijing Institute of Nanoenergy and Nanosystems, Chinese Academy of Sciences, Beijing 100083, P. R. China; School of Nanoscience and Technology, University of Chinese Academy of Sciences, Beijing 100049, P. R. China

Mingli Zheng – Beijing Institute of Nanoenergy and Nanosystems, Chinese Academy of Sciences, Beijing 100083, P. R. China; School of Nanoscience and Technology, University of Chinese Academy of Sciences, Beijing 100049, P. R. China

Complete contact information is available at: <https://pubs.acs.org/10.1021/acs.jpcc.1c03483>

Notes

The authors declare no competing financial interest.

ACKNOWLEDGMENTS

This work was supported by the National Key R & D Project from Minister of Science and Technology (2016YFA0202704) and the National Natural Science Foundation of China (Grant 52005044).

REFERENCES

- (1) Lin, S.; Xu, L.; Xu, C.; Chen, X.; Wang, A.; Zhang, B.; Lin, P.; Yang, Y.; Zhao, H.; Wang, Z. L. Electron transfer in nanoscale contact electrification: effect of temperature in the metal–dielectric case. *Adv. Mater.* **2019**, *31*, 1808197.
- (2) Nie, J.; Wang, Z.; Ren, Z.; Li, S.; Chen, X.; Wang, Z. L. Power Generation from the Interaction of a Liquid Droplet and a Liquid Membrane. *Nat. Commun.* **2019**, *10*, 2264.
- (3) Lin, Z.; Cheng, G.; Lee, S.; Pradel, K.; Wang, Z. L. Harvesting water drop energy by a sequential contact-electrification and electrostatic-induction process. *Adv. Mater.* **2014**, *26*, 4690–4696.
- (4) Liu, X.; Cheng, K.; Cui, P.; Qi, H.; Qin, H.; Gu, G.; Shang, W.; Wang, S.; Cheng, G.; Du, Z. Hybrid energy harvester with bifunctional nano-wrinkled anti-reflective PDMS film for enhancing energies conversion from sunlight and raindrops. *Nano Energy* **2019**, *66*, 104188.
- (5) Le, C.; Vo, C.; Nguyen, T.; Vu, D.; Ahn, K. Liquid–solid contact electrification based on discontinuous-conduction triboelectric nanogenerator induced by radially symmetrical structure. *Nano Energy* **2021**, *80*, 105571.
- (6) Cho, H.; Chung, J.; Shin, G.; Sim, J.; Kim, D.; Lee, S.; Hwang, W. Toward sustainable output generation of liquid–solid contact triboelectric nanogenerators: the role of hierarchical structures. *Nano Energy* **2019**, *56*, 56–64.
- (7) Lin, Z.; Cheng, G.; Lin, L.; Lee, S.; Wang, Z. L. Water–solid surface contact electrification and its use for harvesting liquid-wave energy. *Angew. Chem., Int. Ed.* **2013**, *52*, 12545–12549.
- (8) Yang, X.; Chan, S.; Wang, L.; Daoud, W. Water tank triboelectric nanogenerator for efficient harvesting of water wave energy over a broad frequency range. *Nano Energy* **2018**, *44*, 388–398.
- (9) Ha, J.; Chung, J.; Kim, S.; Kim, J.; Shin, S.; Park, J.; Lee, S.; Kim, J. Transfer-printable micropatterned fluoropolymer-based triboelectric nanogenerator. *Nano Energy* **2017**, *36*, 126–133.
- (10) Lin, S.; Xu, L.; Wang, A.; Wang, Z. L. Quantifying electron-transfer in liquid–solid contact electrification and the formation of electric double-layer. *Nat. Commun.* **2020**, *11*, 399.
- (11) Nie, J.; Ren, Z.; Xu, L.; Lin, S.; Zhan, F.; Chen, X.; Wang, Z. L. Probing contact-electrification-induced electron and ion transfers at liquid–solid interface. *Adv. Mater.* **2020**, *32*, 1905696.
- (12) Zhan, F.; Wang, A.; Xu, L.; Lin, S.; Shao, J.; Chen, X.; Wang, Z. L. Electron transfer as a liquid droplet contacting a polymer surface. *ACS Nano* **2020**, *14*, 17565–17573.
- (13) Lin, S.; Zheng, M.; Luo, J.; Wang, Z. L. Effects of Surface Functional Groups on Electron Transfer at Liquid–Solid Interfacial Contact Electrification. *ACS Nano* **2020**, *14*, 10733–10741.
- (14) Daiguji, H.; Oka, Y.; Adachi, T.; Shirono, K. Theoretical study on the efficiency of nanofluidic batteries. *Electrochem. Commun.* **2006**, *8*, 1796–1800.
- (15) van der Heyden, F. H. J.; Stein, D.; Dekker, C. Streaming current in a single nanofluidic channel. *Phys. Rev. Lett.* **2005**, *95*, 116104.
- (16) Haldrup, S.; Catalano, J.; Hinge, M.; Jensen, G. V.; Pedersen, J. S.; Bienten, A. Tailoring membrane nanostructure and charge density for high electrokinetic energy conversion efficiency. *ACS Nano* **2016**, *10*, 2415–2423.
- (17) Xu, Y.; Chen, P.; Zhang, J.; Xie, S.; Wan, F.; Deng, J.; Cheng, X.; Hu, Y.; Liao, M.; Wang, B.; et al. A one-dimensional fluidic nanogenerator with a high power conversion efficiency. *Angew. Chem., Int. Ed.* **2017**, *56*, 12940–12945.

- (18) He, S.; Zhang, Y.; Qiu, L.; Zhang, L.; Xie, Y.; Pan, J.; Chen, P.; Wang, B.; Xu, X.; Hu, Y.; et al. Chemical-to-electricity carbon: water device. *Adv. Mater.* **2018**, *30*, 1707635.
- (19) Terris, B. D.; Stern, J. E.; Rugar, D.; Mamin, H. J. Contact electrification using force microscopy. *Phys. Rev. Lett.* **1989**, *63*, 2669.
- (20) Lin, S.; Shao, T. Bipolar charge transfer induced by water: experimental and first-principles studies. *Phys. Chem. Chem. Phys.* **2017**, *19*, 29418.
- (21) Nonnenmacher, M.; O'Boyle, M. P.; Wickramasinghe, H. K. Kelvin probe force microscopy. *Appl. Phys. Lett.* **1991**, *58*, 2921.
- (22) Kilpatrick, J.; Collins, L.; Weber, S.; Rodriguez, J. Quantitative comparison of closed-loop and dual harmonic Kelvin probe force microscopy techniques. *Rev. Sci. Instrum.* **2018**, *89*, 123708.
- (23) Collins, L.; Kilpatrick, J.; Kalinin, S.; Rodriguez, J. Towards nanoscale electrical measurements in liquid by advanced KPFM techniques: a review. *Rep. Prog. Phys.* **2018**, *81*, 086101.
- (24) Collins, L.; Jesse, S.; Kilpatrick, J. I.; Tselev, A.; Varenyk, O.; Okatan, M. B.; Weber, S. A. L.; Kumar, A.; Balke, N.; Kalinin, S. V.; Rodriguez, B. J.; et al. Probing charge screening dynamics and electrochemical processes at the solid-liquid interface with electrochemical force microscopy. *Nat. Commun.* **2014**, *5*, 3871.
- (25) Burgo, T.; Galembeck, F.; Pollack, G. H. Where is water in the triboelectric series? *J. Electrostat.* **2016**, *80*, 30–33.
- (26) Lowell, J. Contact charging: the effect of sample history. *J. Phys. D: Appl. Phys.* **1988**, *21*, 138–147.
- (27) Teschke, O.; de Souza, E. F. Dielectric exchange: the key repulsive or attractive transient forces between atomic force microscope tips and charged surfaces. *Appl. Phys. Lett.* **1999**, *74*, 1755–1757.
- (28) Xu, C.; Zi, Y.; Wang, A.; Zou, H.; Dai, Y.; He, X.; Wang, P.; Wang, Y.; Feng, P.; Li, D.; et al. On the electron-transfer mechanism in the contact-electrification effect. *Adv. Mater.* **2018**, *30*, 1706790.
- (29) Lin, S.; Xu, C.; Xu, L.; Wang, Z. L. The overlapped electron-cloud model for electron transfer in contact electrification. *Adv. Funct. Mater.* **2020**, *30*, 1909724.
- (30) Willatzen, M.; Wang, Z. L. Theory of contact electrification: optical transitions in two-level systems. *Nano Energy* **2018**, *52*, 517–523.
- (31) Wang, Z. L.; Wang, A. On the origin of contact-electrification. *Mater. Today* **2019**, *30*, 34–51.
- (32) Singh, H.; Khare, N. Improved performance of ferroelectric nanocomposite flexible film based triboelectric nanogenerator by controlling surface morphology, polarizability, and hydrophobicity. *Energy* **2019**, *178*, 765–771.